INTERNATIONAL JOURNAL OF
ENERGY AND ENVIRONMENT

Volume 7, Issue 4, 2016 pp303-316
Journal homepage: www.IJEE.IEEFoundation.org

Numerical simulation and analyses for sinter cooling process with convective and radiative heat transfer

Xun Shen [1,2,3], Lingen Chen [1,2,3], Shaojun Xia [1,2,3], Fengrui Sun [1,2,3]

[1] Institute of Thermal Science and Power Engineering, Naval University of Engineering, Wuhan 430033, China.
[2] Military Key Laboratory for Naval Ship Power Engineering, Naval University of Engineering, Wuhan 430033, China.
[3] College of Power Engineering, Naval University of Engineering, Wuhan 430033, China.

Abstract
Based on the numerical heat transfer theory, a two-dimensional unsteady model for sinter cooling process is established by applying porous medium flow and heat transfer mechanism. The complex heat transfer process, including three modes of heat conduction inside the sinter ore particles, gas-solid convection and radiation in the trolley, is taken into account. By using the mass, momentum and energy conservation equations, the pressure field, temperature distribution and the temperature characteristic of outlet gas are obtained by the numerical simulation method. The effect of radiative heat transfer on the cooling process is analyzed.

Keywords: Sinter ore; Complex heat transfer; Flow and heat transfer; Numerical simulation.

1. Introduction
The iron and steel industry is key to China's economy. It's also an energy intensive industry with complex processes, consumption of natural resources and energy, and emissions of waste materials [1-20]. The iron and steel industry consumes more than 10% of national energy. The sintering process uses about 15% of whole energy consumption in an iron and steel plant, second only to the ironmaking process [21]. The energy consumption processes occurs in two major metallurgical pieces of equipment: a sintering machine and an annular cooler. Fluid flow and heat transfer processes occur in the annular cooler, which is a key thermal process device. The flow and heat transfer processes in the trolley are porous medium cross-flow and heat exchange processes [22].
The development of modern computing technology has provided a strong means of analyzing the mathematical models of metallurgical processes [23]. Some scholars have done extensive research on simulations of the annular cooling process. Minoura et al. [24] took account for the heat conduction within the sinter ore particles, gas distribution, particle diameter segregation, and initial temperature of sinter bed, and established a 2-dimensional heat exchanger model to estimate the heat exchange performance of the sinter cooling process. Jang et al. [25] developed a 3-dimensional unsteady fixed bed model with a packed 4-row spheres bed. With the sinter ore simplified as spheres, the turbulent flow and heat exchange in the sinter bed were simulated. Caputo et al. [26] simplified the sinter bed as a matrix of cross-flow heat exchangers and established a dynamic model for the sinter cooling process for the

optimization of heat recovery. Based on the VS platform simulation, analyses were made with different operating parameters. Leong et al. [27] established a sinter cooling model with inclined air passage and different distributions of sinter porosity. Based on local equilibrium thermodynamics, the effects of different porosity distributions in vertical and transversal directions on the flow and temperature fields were investigated. Zhang et al. [28] developed one-dimensional unsteady mathematical model for the gas-solid heat transfer process of high temperature, and simulated the process based on the TDMA and iteration methods. Zhang et al. [29-32] adopted the two energy equations mode to simulate the sinter cooling process in a single trolley and obtained the average temperatures of sinter ore and outlet gas. The effects of five main parameters on the process performance were investigated and optimization of those relevant parameters was carried out. Xia and Zeng [33] developed one-dimensional unsteady mathematical model of trolley cross-section based on local equilibrium thermodynamics. Based on Ref. [33], Liu et al. [34] made a further investigation of air density distribution and temperature fields with linear porosity segregation under Coriolis force. The effect of porosity segregation on the temperature uniformity of the sinter bed was analyzed.
The simulations of annular cooling process made by Refs. [24-34] only took into account the factor of convective heat transfer. Some of those investigated the effect of heat conduction inside the sinter ore particles. However, the heat radiation factor has rarely been taken into account. Accounting for the high temperature of sinter ore, the heat transfer should be compound, as mentioned in Ref. [35], and radiation must be taken into consideration. This paper will establish a two-dimensional unsteady model of cooling process in a 415 m^3 annular cooler. Three modes of heat conduction inside the sinter ore particles, gas-solid convection and radiation in the trolley will be taken into account. By numerical simulation, the pressure and temperature fields of fluid, and the temperature field of sinter ore will be obtained. The effect of heat radiation factor on temperature field inside the sinter ore and temperature distribution of outlet gas will be analyzed as well.

2. Model of sinter ore cooling process

2.1 Model and assumptions

As shown in Figure 1, a sinter ore cooling process is considered as a continuous process. On the effective cooling orbit, the cooling air flows across the sinter ore. The sinter inlet flow velocity is a constant $\vec{V}_s$. The flow velocity of inlet air is also a constant $\vec{V}_{gi}$. There are no chemical reaction in the cross-flow process.

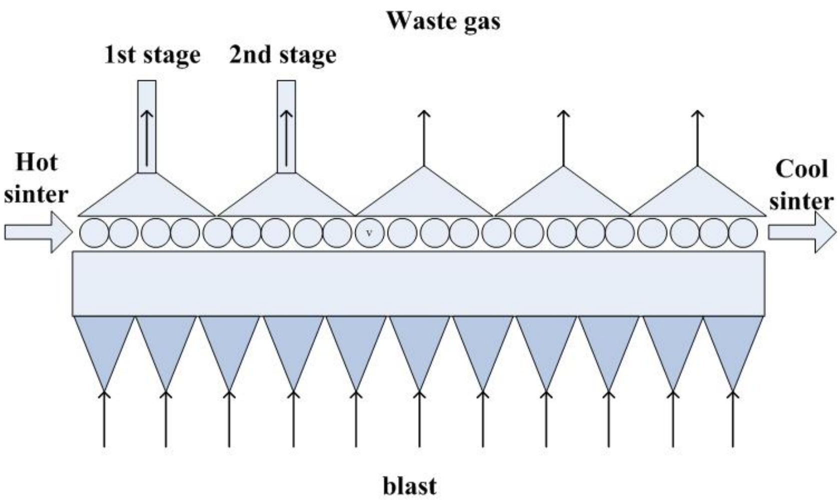

Figure 1. Continuous cooling process of sinter ore

Heat transfer in porous media is relatively complex, including heat conduction inside particles, contact heat conduction, gap air heat conduction, heat convection and heat radiation. Taking the complexity of the actual process into consideration, this paper makes the following assumptions: (1) Unlike Refs.[25-34] which only involve convection, this paper considers three modes of heat transfer, including heat conduction inside particles, heat convection and heat radiation; (2) The cooling system operates on a

stable basis, the bed is even, and the structural and operational parameters are constants; (3) Sinter ore particle moves flatly; (4) There is no backflow or heat conduction for cooling gas; (5) There is no heat transfer in the width or length direction or, rather, all the parameters are uniform in the cross section.
Based on the assumptions mentioned above, the model of sinter ore cooling process becomes a two-dimensional one. It is assumed that the moving bed consists of a series of fixed beds [36], whose positions change with cooling time, as shown in Figure 2.

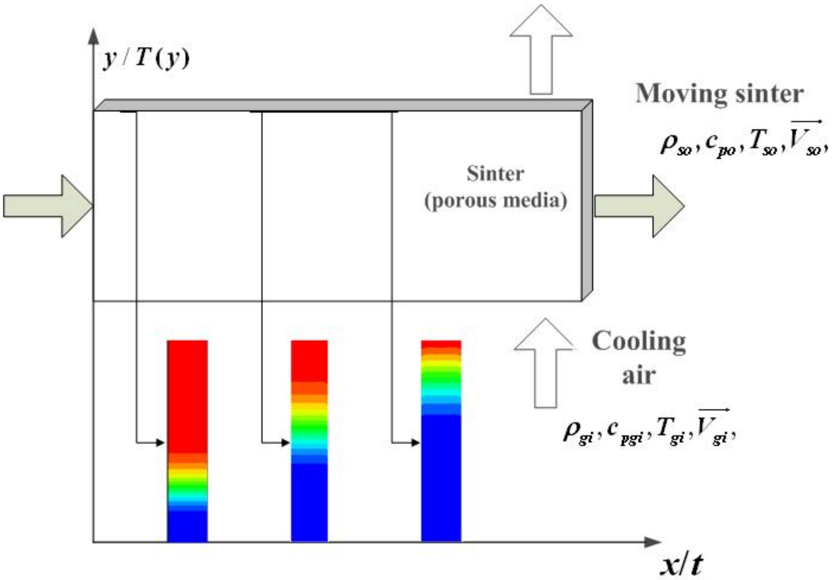

Figure 2. Two-dimensional unsteady model of continuous cooling process of sinter ore

Based on the porous medium theory and the corresponding two-dimensional unsteady mathematical model [37], the governing equations for elementary unit of the bed are as follows:
Continuity equation (for cooling air):

$$\frac{\partial\left(\varepsilon\rho_g\right)}{\partial t}+\nabla\cdot\left(\rho_g\overrightarrow{V_g}\right)=0 \tag{1}$$

Momentum equation (for cooling air):

$$\frac{\partial\left(\rho_g\overrightarrow{V_g}\right)}{\partial t}+\overrightarrow{V_g}\cdot\nabla\cdot\left(\rho_g\overrightarrow{V_g}\right)=\rho_g\vec{g}-\nabla p+\nabla\cdot\vec{\tau}-\vec{S} \tag{2}$$

where $\vec{S}$ is the momentum loss source consisting of both viscosity loss and inertia loss. It is given by the modified Darcy's Law [37]:

$$S=\frac{\mu}{\alpha}\overrightarrow{V_g}+\frac{C_2}{2}\left(\rho_g\left|\overrightarrow{V_g}\right|\right)\overrightarrow{V_g} \tag{3}$$

where μ is the kinematic viscosity, α is the permeability of porous media, $1/\alpha$ and C_2 are the coefficients of viscosity resistance and inertia resistance, respectively. They are given by the Ergun equation [38]:

$$\frac{1}{\alpha}=\frac{150}{\varepsilon^3}\frac{(1-\varepsilon)^2}{\phi^2 d^2},\ C_2=\frac{7}{2\varepsilon^3}\frac{1-\varepsilon}{\phi d} \tag{4}$$

In the sinter ore bed, because of local non-equilibrium thermodynamic property, the sinter temperature T_s is different from the air temperature T_g. Then, the two energy equations should be adopted:
Energy equation for sinter:

$$\left(1-\varepsilon\right)\frac{\partial\left(\rho_s c_s T_s\right)}{\partial t}=\left(1-\varepsilon\right)\nabla\cdot\left(k_s T_s\right)+hA\left(T_g-T_s\right)+\varepsilon_r\sigma A\left(T^4{}_g-T^4{}_s\right) \tag{5}$$

Energy equation for air:

$$\frac{\partial\left(\varepsilon c_g\rho_g T_g\right)}{\partial t}+\overrightarrow{V_g}\cdot\nabla\cdot\left(c_g\rho_g T_g\right)=\varepsilon\nabla\cdot\left(k_g T_g\right)+hA\left(T_s-T_g\right)+\varepsilon_r\sigma A\left(T^4{}_s-T^4{}_g\right) \tag{6}$$

where A is the specific surface area to volume, and it is given by the Achenbach's criterion [39]:

$$A=6\left(1-\varepsilon\right)/d \tag{7}$$

Because of the large size, a big temperature difference inside sinter particles exists. An equivalent convective heat transfer coefficient h_c is introduced to eliminate the influence of heat conduction inside sinter particles. For the metallurgic production, the general expression of h_c is [40]:

$$h_c=h/b=\frac{k_g Nu}{bd}=\frac{k_g(2+0.6\,\mathrm{Re}^{0.5}\,\mathrm{Pr}^{0.33})}{(1+Bi/5)d} \tag{8}$$

where Nu is the Nusselt number and given by the Rows expression [41]:

$$Nu=2+0.6\,\mathrm{Re}^{0.5}\,\mathrm{Pr}^{0.33} \tag{9}$$

Radiative heat transfer is a significant factor for the sinter cooling process, and can be described with heat transfer ratio e, which is defined as the ratio of radiative heat transfer to convection heat transfer. It is defined as:

$$e=\frac{\varepsilon_r\sigma A\left(T^4{}_s-T^4{}_g\right)}{h_c A\left(T_s-T_g\right)}=\frac{\varepsilon_r\sigma\left(T^2{}_s+T^2{}_g\right)\left(T_s+T_g\right)}{h_c}=\frac{h_r}{h_c} \tag{10}$$

When heat transfer ratio e equals to 0, it means that there only exists convective heat transfer between sinter and cooling air.
Combining Eqs. (5), (6), (8) with (9) gives the two energy equations:

$$\left(1-\varepsilon\right)\frac{\partial\left(\rho_s c_s T_s\right)}{\partial t}=\left(1+e\right)h_c A\left(T_g-T_s\right) \tag{11}$$

$$\frac{\partial\left(\varepsilon c_g\rho_g T_g\right)}{\partial t}+\overrightarrow{V_g}\cdot\nabla\cdot\left(c_g\rho_g T_g\right)=\left(1+e\right)h_c A\left(T_s-T_g\right) \tag{12}$$

The initial condition is: $T_s=T_{s0}$.
The boundary conditions are given as:
At the air inlet: $\overrightarrow{V_g}=\overrightarrow{V_{gi}}, T_g=T_{gi}$;
At the air outlet: both pressure outlet and outflow are accepted. The pressure difference is given by actual measured value.

2.2 Parameter settings
The effect factors on the sinter cooling process consist of both physical property parameters and processing parameters. It is assumed that there does not exist any reaction in the cooling process, so the density of sinter ore is set as a constant (3000kg/m$^{3)}$ and that of the cooling air is 1.205kg/m^3, but both of the heat capacities of the sinter ore and the air vary with the temperature [42]. The fixed parameters and equations for the sinter cooling process calculations of a 415 m^2 annular cooler are listed in Table 1.

Table 1. Fixed parameters and equations in the calculations

	Major parameters		Values
Sinter ore	Density	kg/m³	3000
	Heat Capacity	J/(kg·K)	$752.4+0.26T_s$
	Height	M	1.5
	Cooling length	M	120
	Porosity	—	0.4
	Mean radius	M	0.1
	Inlet temperature	K	1023
Air	Inlet velocity	m/s	1.5
	Inlet temperature	K	300
	Density	kg/m³	1.205
	Heat Capacity	J/(kg·K)	$919.6+0.3T_g-6.69\times10^{-5}T_g^2$

2.3 Numerical simulation
The mathematical model is solved in the platform of computational fluid dynamics software ANSYS FLUENT 14.0. To complete the numerical simulation, a two-dimensional rectangular radial section, with the length $H = 1.5\text{m}$ and the width of $l = 0.3\text{m}$, is chosen. The section is meshed in 150×30 grids. The results show that double mesh intensity has little effect on the simulation result with a relative error less than 0.1%. FLUENT soft solves the energy equations based on local equilibrium thermodynamics. Because the heat transfer coefficients are limited and the densities of air and sinter ore are significantly different in the actual cooling process, the two energy equations based on the local non-equilibrium thermodynamics are applied. User defined scalars (UDS) are adopted to solve T_s and T_g. At the same time, as the trolley moves at a given velocity, the location of sinter bed can be replaced by the cooling time, and then the characteristics changes with the cooling time. The velocity-pressure coupled SIMPLE algorithm in second order implicit discrete form is selected. As the air inlet velocity is $\overrightarrow{V_{gi}} = 1.5\text{m/s}$, and the height of sinter bed is also only $H = 1.5\text{m}$, the time step is set as $\Delta t = 0.01\text{s}$ to control the accuracy.

3. Numerical examples and analyses
3.1 Modeling verification
Table 2 lists some major device and operating parameters of a 415 m^2 annular cooler in an iron and steel plant. With the fixed parameters and equations listed in Table 1 and the heat transfer ratio varying from 0 to 0.1, the gas flow velocities, pressure distributions and temperature fields of entire cooling process are obtained. The average temperatures of outlet air at the first and second stages and the outlet of the sinter are compared with the actual situation.
Table 3 lists the average temperatures of outlet air at the first and second stages and the outlet of the sinter. It can be seen that when the heat transfer ratio increases from 0 to 0.1, the temperature of the sinter outlet decreases, and both the average temperatures of outlet air at the first and second stages increase, respectively. Moreover, Table 2 and Table 3 show that in the numerical simulations of different heat transfer ratio, all the temperatures of outlet sinter meet the actual production datum: T_{so} < 393K, the average temperatures of outlet air at the first stage are in the range between 633K and 693K, and those at the second stage are in the range between 470K and 535K.

Table 2. Device and operation parameters of 415 m^2 annual cooler

Device and operation parameters		Values
Effective cooling area	m^2	415
Width of trolley	m	3.5
Height of baffle plate	m	1.6
Velocity of trolley	m/s	0.033
Cooling time	s	3600
Pressure drop	Pa	670~710
Temperature of inlet sinter	K	1023~1123
Temperature of outlet sinter	K	<393
Average temperature of outlet air at the first stage	K	630~695
Average temperature of outlet air at the second stage	K	470~535

Table 3. Temperatures of sinter ore at outlet and gas of 1st and 2nd stage

heat transfer ratio	0	0.05	0.1
Temperature of outlet sinter /K	382.94	373.72	369.77
Average temperature of outlet air at the first stage /K	657.29	674.31	680.18
Average temperature of outlet air at the second stage /K	525.88	528.99	530.05

3.2 Analyses of simulation results

Figure 3 shows the gas flow and pressure distribution contour inside the sintered bed. Figure 4 shows the gas pressure corresponding to height of sinter bed. It can be seen that when the air flows cross the bed, its pressure drops approximately 687.4 Pa, namely, the air pressure drop is in the actual range between 670 Pa and 710 Pa. As the flow resistance and heat transfer of air inside the bed are independent, the gas flow and pressure distribution of air do not change with the heat transfer ratio e. The velocity vector keeps constant and the pressure decreases linearly with the height of bed.

Figures 5-7 show the solid and gas temperature distribution contours inside the sintered bed with $e = 0$, $e = 0.05$ and $e = 0.1$, respectively. It can be seen that during the early stage (about the early 1800s), the temperature of sinter decreases rapidly due to the large temperature difference between gas and solid. And during the following cooling time, it changes relatively slowly. So the early stage is the key one for sinter cooling process. When the heat transfer ratio increases, the heat exchange is strengthened: the temperature of sinter decreases more rapidly; the temperature of gas inside the bed has a more significant increment and steeper temperature gradient during the early stage. While both the temperature increment and gradient of gas decrease at the following stage of cooling process, and the solid and gas temperature distributions at different heat transfer ratios are similar.

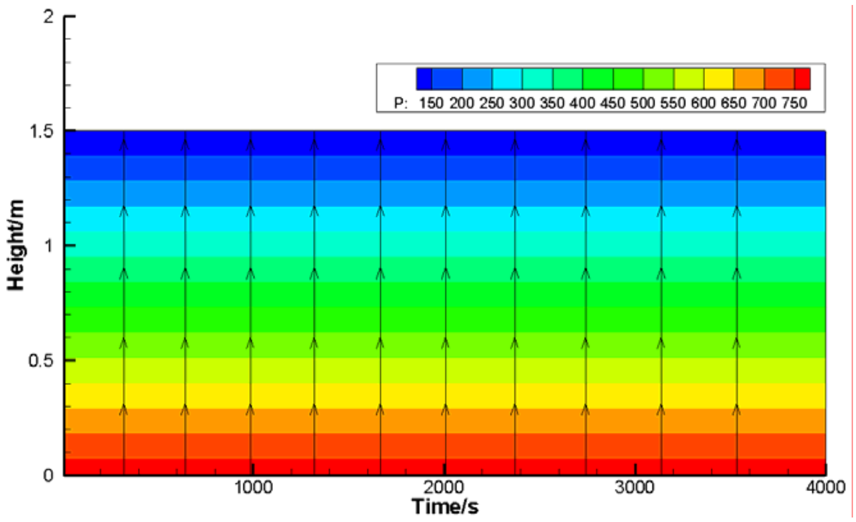

Figure 3. Pressure distribution contour of gas inside sintered bed

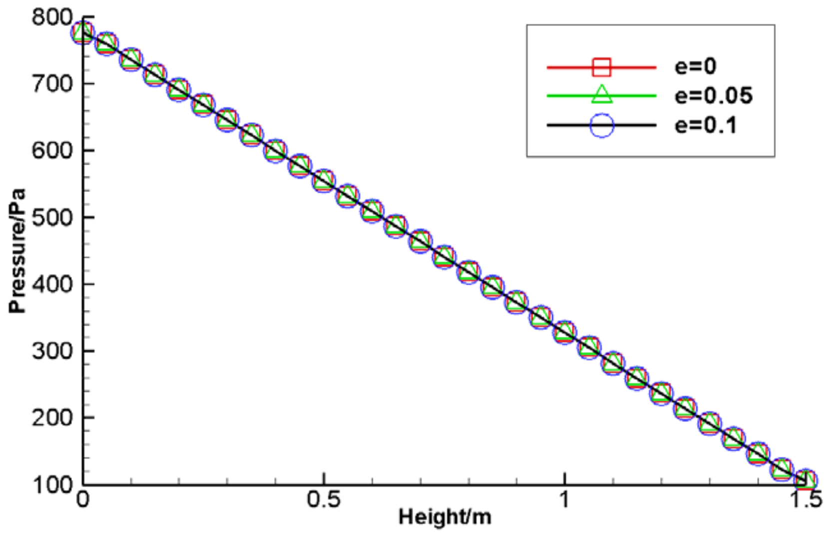

Figure 4. Pressure of gas inside sintered bed versus height

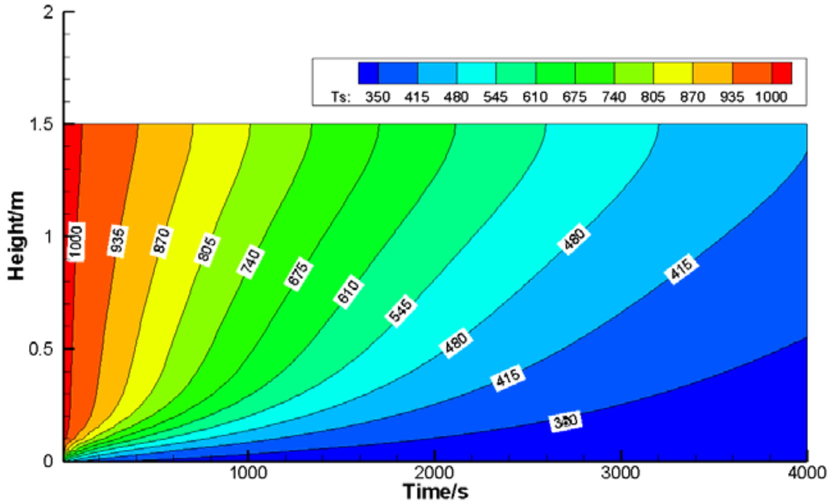

(a) Solid

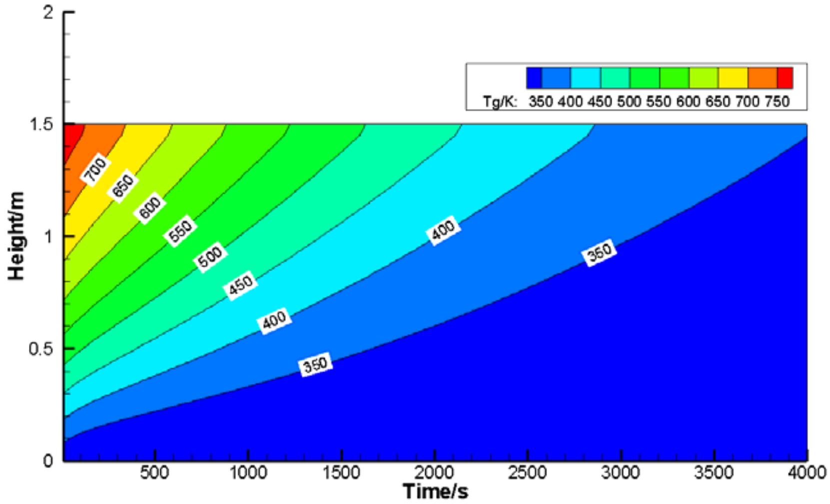

(b) Gas

Figure 5. Solid/gas temperature distribution contours inside sintered bed with $e = 0$

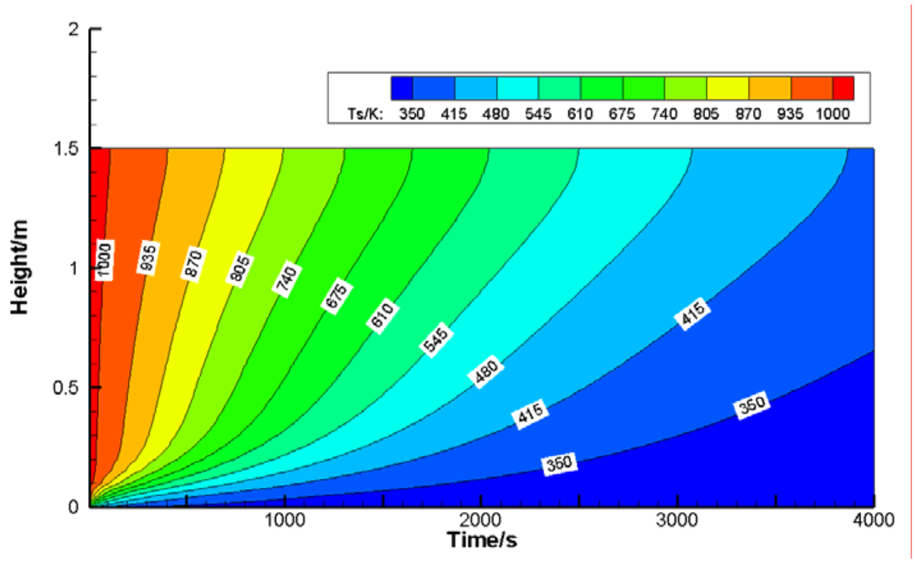

(a) Solid

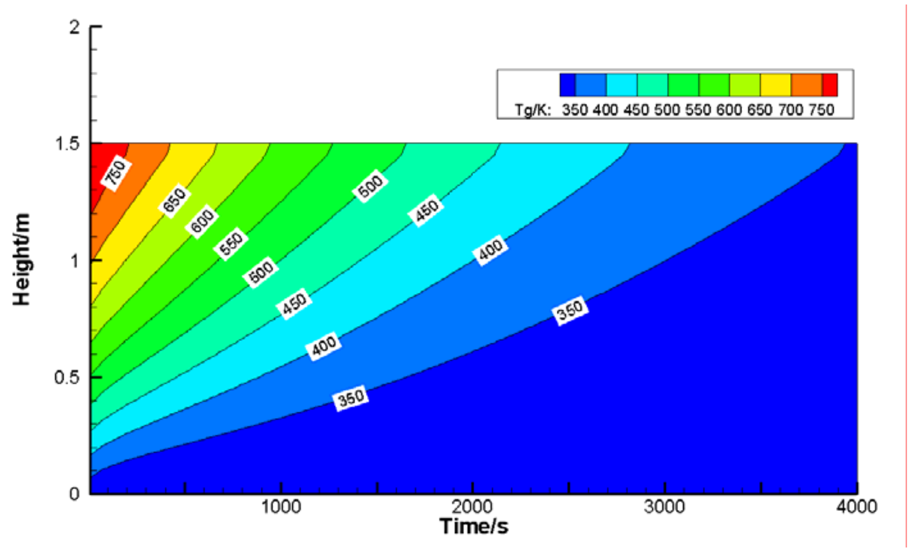

(b) Gas

Figure 6. Solid/gas temperature distribution contours inside sintered bed at $e = 0.05$

Figures 8-10 show effects of the heat transfer ratio e on temperatures of sintered bed at different heights. Obviously, at the same heat transfer ratio, the temperature drop of the sinter bed becomes smaller with the increase of height. And the temperature drop rate is also different from at different height. The temperature of the sinter bed decreases rapidly at the forepart cooling time at the lower height; the temperature drop rate slows up gradually. Compared with the middle and bottom bed, the temperature drop rate of the upper bed is relatively slow. At the same height, the temperature of the sinter bed decreases with the increase of heat transfer ratio e but the amplitude of temperature drop slows. The effect of the heat transfer ratio e on the temperature of sinter seems to be very small at the early stage of the cooling process for different height. Specifically, the early stages for $H = 0.25\text{m}$, $H = 0.75\text{m}$ and $H = 1.25\text{m}$ are in the early 400s, 600s and 1000s, respectively.
Figure 11 shows the effect of the heat transfer ratio e on the temperature of outlet gas. It can be seen that the temperature of outlet gas decreases when the cooling time increases, and the temperature drop slows at the same time. As the cooling process proceeds, the temperature of the sinter decreases. It shows that the temperature difference between the air and sinter becomes smaller, and that the heat transfer

weakens. During the early stage of the cooling process, namely the early 1800s, the temperature of outlet gas increases when the heat transfer ratio e increases. During the following cooling time, on the contrary, the temperature decreases. It is because that during the early stage, the temperature difference makes drastic heat transfer between air and sinter, increasing heat transfer ratio leads to the increase of temperature of outlet gas. At the later stage, the heat transfer is limited by the relatively small temperature difference, so the temperature of outlet gas increases less. Therefore, for reinforcing the exhaust heat of the sinter cooling process, the early stage is the key period, namely to enhance heat transfer at the first and second stages.

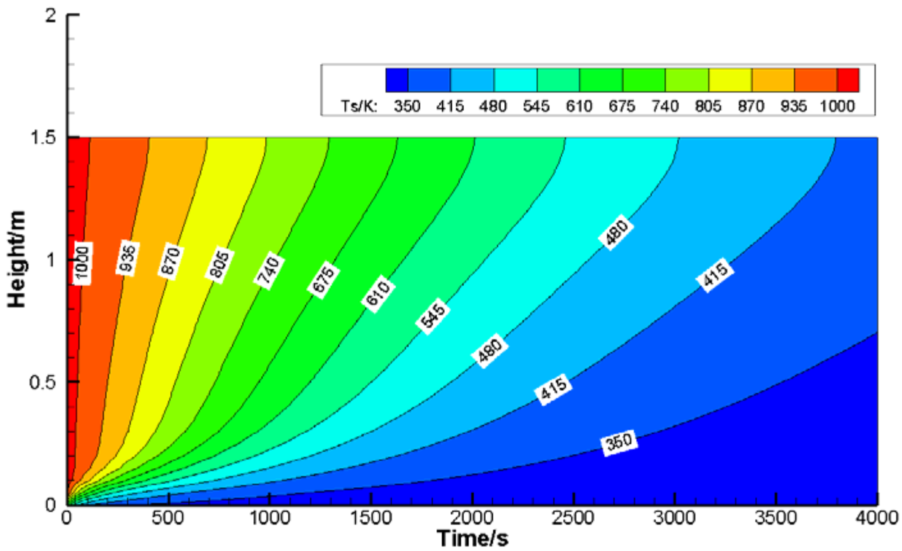

(a) Solid

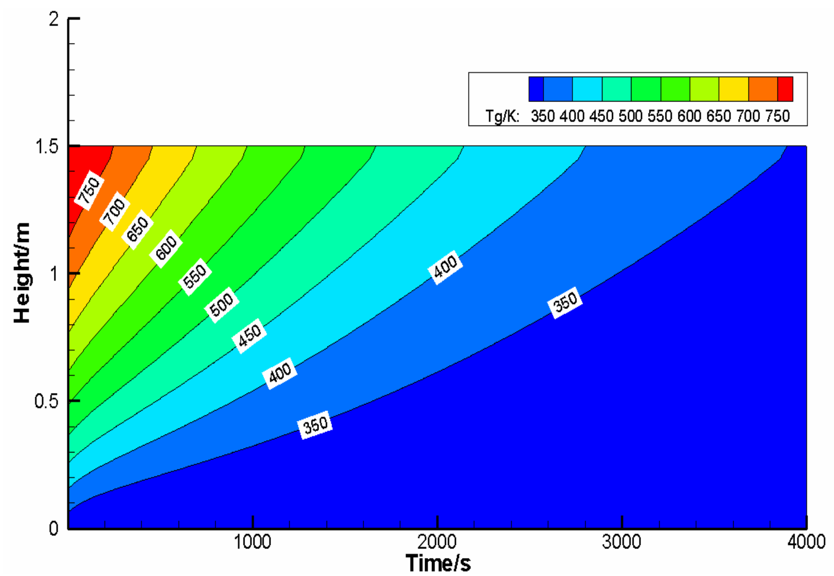

(b) Gas

Figure 7. Solid/gas temperature distribution contours inside sintered bed with $e = 0.1$

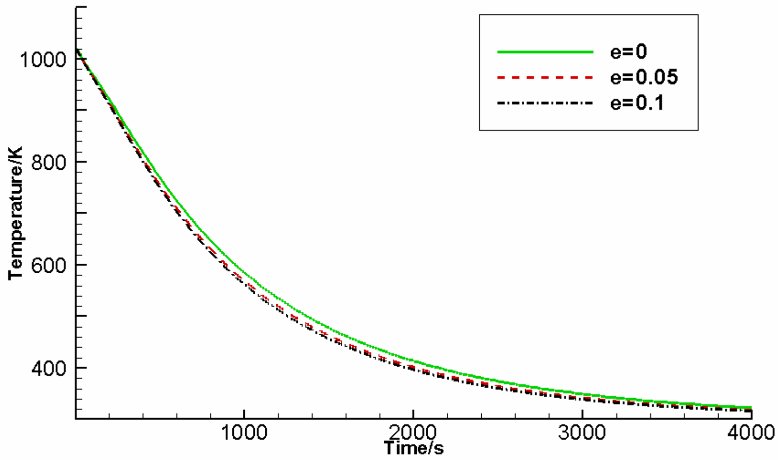

Figure 8. Effect of heat transfer ratio e on temperature of sintered bed at $H = 0.25\text{m}$

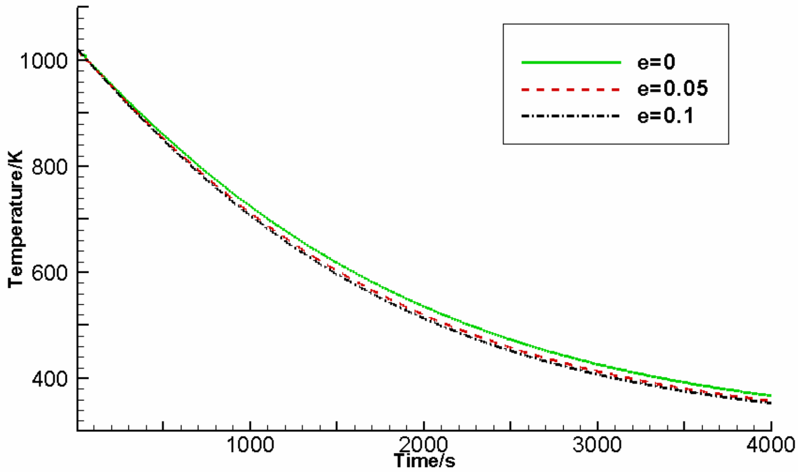

Figure 9. Effect of heat transfer ratio e on temperature of sintered bed at $H = 0.75\text{m}$

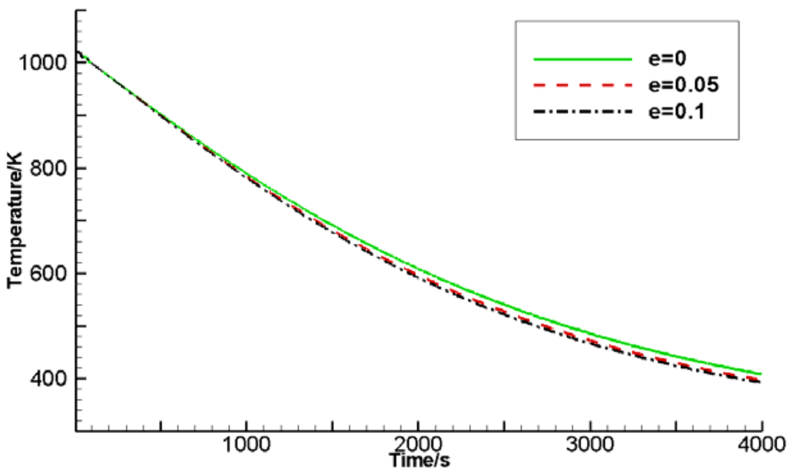

Figure 10. Effect of heat transfer ratio e on temperature of sintered bed at $H = 1.25\text{m}$

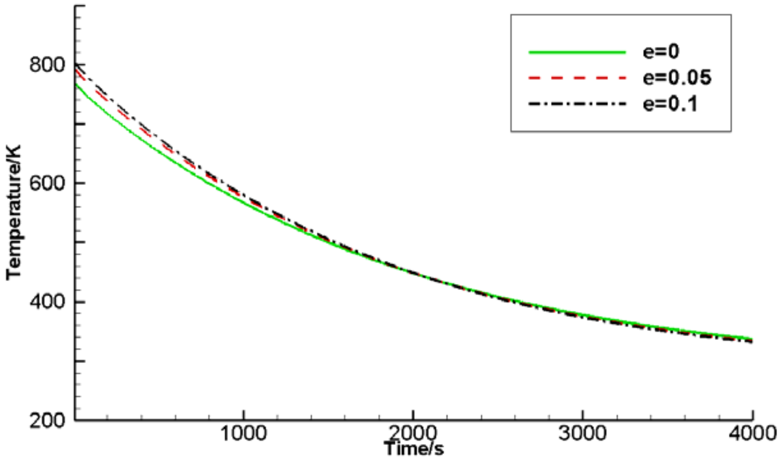

Figure 11. Effect of heat transfer ratio e on temperature of waste gas

4. Conclusion

A two-dimensional unsteady model for sinter cooling process is established based on the actual sinter cooling process in an annular cooler. The complex heat transfer process, including three modes of heat conduction inside the sinter ore particles, gas-solid convection and radiation in the trolley, is taken into account. The heat transfer ratio is proposed to explore the effect of heat radiation to the cooling process. With actual device and operating parameters, modeling verification and analyses of datum based on numerical simulation are conducted. The results are consistent with actual production datum when the heat transfer ratio e varies from 0 to 0.1. The pressure field, temperature distribution and the temperature characteristic of outlet gas are obtained by numerical simulation method. The effect of radiative heat transfer on the cooling process is analyzed. The results show that the heat transfer ratio e has no effect on the gas flow and pressure distribution of air. The increase of the ratio e can reinforce the heat transfer between the sinter and air, which will lead to bigger increase of temperature drop rate of the sinter. The solid and gas temperature distribution trends at different heat transfer ratios are similar. The results obtained herein may provide some guidelines for the research on the actual cooling process in an annular cooler.

Nomenclature

A	specific surface area ($\mathrm{m^{-1}}$)
Bi	Biot number
C	inertia resistance coefficient ($\mathrm{m^{-1}}$)
c	specific heat capacity ($\mathrm{J/kg \cdot K}$)
d	particle diameter (m)
e	heat transfer ratio
g	gravity vector ($\mathrm{m^2/s}$)
H	height (m)
h	heat transfer coefficient ($\mathrm{W/m^2 \cdot K}$)
k	apparent thermal conductance ($\mathrm{W/m \cdot K}$)
L	length (m)
Nu	Nusselt number
P	pressure (Pa)
Pr	Prandlt number
Re	Reynolds number
S	source of momentum loss ($\mathrm{kg/(m^2 \cdot s^2)}$)
T	thermodynamic temperature (K)
t	time (s)
V	velocity (m/s)

Greek letters

ε	porosity ; emissivity
ρ	density ($\mathrm{kg/m^3}$)
τ	viscous stress tensor
μ	kinematic viscosity ($\mathrm{Pa \cdot s}$)
α	permeability ($\mathrm{m^2}$)
ϕ	shape factor of particle
σ	blackbody radiation constant ($\mathrm{W/(m^2 \cdot K^4)}$)

Subscripts

c	(equivalent) convection
g	gas
i	input
o	output
r	radiation
s	solid
0	initial (value)

Acknowledgements
This paper is supported by the National Key Basic Research and Development Program of China (973) (Project No. 2012CB720405) and the National Nature Science Foundation of Naval University of Engineering (No. HG DYDJJ-13002).

References
[1] Yin R. Metallurgical Process Engineering. Berlin: Springer, 2006.
[2] Yin R. Essence, function of steel production process and future development model of steel plant. Science in China Series E: Technological Sciences, 2008, 38(9): 1365-1377. (in Chinese).
[3] Cai J, Wang J, Chen C. Recovery of residual-heat integrated steelworks. Iron and Steel, 2007, 42(6): 1-7. (in Chinese).
[4] Sun W, Cai J, Ye Z. Advances in energy conservation of China steel industry. The Scientific World Journal, 2013: 1-8.
[5] Zhang H, Dong L, Li H, Chen B. Investigation of the residual heat recovery and carbon emission mitigation potential in a Chinese steelmaking plant: A hybrid material/energy flow analysis case study. Sustainable Energy Technologies and Assessments, 2013, 2: 67-80.
[6] Wübbeke J, Heroth T. Challenges and political solutions for steel recycling in China. Resource Conservation of Recycling, 2014, 87: 1-7.
[7] Meng F K, Chen L G, Sun F R, Yang B. Thermoelectric power generation driven by blast furnace slag flushing water. Energy, 2014, 66: 965-972.
[8] Xiong B, Chen L G, Meng F K, Sun F R. Modeling and performance analysis of a two-stage thermoelectric energy harvesting system from blast furnace slag water waste heat. Energy, 2014, 77: 562-569.
[9] Feng H J, Chen L G, Xie Z H, Ding Z M, Sun F R. Generalized constructal optimization for secondary cooling process of slab continuous casting based on entransy theory. Science China: Technological Sciences, 2014, 57(4): 784-795.
[10] Feng H J, Chen L G, Xie Z H, Sun F R. Constructal entransy optimizations for insulation layer of steel rolling reheating furnace wall with convective and radiative boundary conditions. Chinese Science Bulletin, 2014, 59(20): 2470-2477.
[11] Zhang Z L, Chen L G, Ge Y L, Sun F R. Thermodynamic analysis for a regenerative gas turbine cycle in coking process. International Journal of Energy and Environment, 2014, 5(6): 701-708.
[12] Feng H J, Chen L G, Xie Z H, Sun F R. Constructal entransy dissipation rate minimization for variable cross-section insulation layer of the steel rolling reheating furnace wall. International Communication of Heat and Mass Transfer, 2014, 52: 26-32.
[13] Feng H J, Chen L G, Xie Z H, Ding Z M, Sun F R. Generalized constructal optimization for solidification heat transfer process of slab continuous casting based on heat loss rate. Energy, 2014, 66: 991-998.
[14] Liu X, Qin X Y, Chen L G, Sun F R. CO2 emission optimization for a blast furnace considering plastic injection. International Journal of Energy and Environment, 2015, 6(2): 175-190.
[15] Liu C X, Xie Z H, Sun F R, Chen L G. System dynamics analysis on characteristics of iron-flow in sintering process. Applied Thermal Engineering, 2015, 82: 206-211.
[16] Chen L G, Yang B, Shen X, Xie Z H, Sun F R. Thermodynamic optimization opportunities for the recovery and utilization of residual energy and heat in China steel industry: A case study. Applied Thermal Engineering, 2015, 86: 151-160.
[17] Zhang Z L, Chen L G, Ge Y L, Sun F R. Thermodynamic analysis of an air Brayton cycle for recovering waste heat of BF slag. Applied Thermal Engineering, 2015, 90: 742-748.
[18] Liu X , Chen L G, Qin X Y, Sun F R. Exergy loss minimization for a blast furnace with comparative analyses for energy flows and exergy flows. Energy, 2015, 93: 10-19.
[19] Liu X, Chen L G, Feng H J, Sun F R. Constructal design for blast furnace wall based on the entransy theory. Applied Thermal Engineering, in press.
[20] Feng H J, Chen L G, Xie Z H, Sun F R. Constructal designs for insulation layers of steel rolling reheating furnace wall with convective and radiative boundary conditions. Applied Thermal Engineering, in press.
[21] Wei J. Energy strategy in iron & steel enterprises. Energy for Metallurgical Industry, 2007, 26(2): 3-6, 11. (in Chinese).
[22] Randall M G. Sintering Theory and Practice. New York: Wiley-Interscience, 1996.

[23] Chen L G, Xia S J, Xie Z H, Liu X W, Shen X, Sun F R. Progress in study on dynamic mathematical modeling of iron and steel metallurgy processes. Journal of Thermal Science and Technology, 2014, 13(2): 95-125. (In Chinese).
[24] Minoura T, Sakamono Y, Hashimoto K. Heat transfer and fluid flow analysis of sinter coolers with considerations of size segregation and initial temperature distribution. Heat Transfer- Japanese Research, 1990, 19(6): 537-555.
[25] Jang J Y, Chiu Y W. 3-D transient conjugated heat transfer and fluid flow analysis for the cooling process of sintered bed. Applied Thermal Engineering, 2009, 29(14): 2895-2903.
[26] Caputo A C, Cardarelli G, Pelagagge P. Analysis of heat recovery in gas-solid moving beds using a simulation approach. Applied Thermal Engineering, 1996, 16(1): 89-99.
[27] Leong J C, Jin K W, Shiau J S. Effect of sinter layer porosity distribution on flow and temperature fields a sinter cooler. International Journal of Minerals, Metallurgy and Materials, 2009, 16(3): 265-272.
[28] Zhang X, Wen Z, Lou G. Numerical simulation and parameters analysis on the gas-solid heat transfer process of high temperature sinter. Journal of University of Science and Technology Beijing, 2011, 33(3): 339-345. (in Chinese).
[29] Zhang X, Zhang J, Dai C. Optimization and simulation of sinter cooling process. Journal of Chemical Industry and Engineering (China), 2011, 62(11): 3081-3087. (in Chinese).
[30] Zhang J, Zhang X, Zhou J. Optimal orthogonal simulation research of sinter cooling. Iron and Steel, 2011, 46(7): 86-89. (in Chinese).
[31] Zhang J, Tian W, Dai C. Simulation and optimization of sinter circular cooler layer-loading. Journal of Chemical Industry and Engineering (China), 2012, 63(5): 1385-1390. (in Chinese).
[32] Li M, Mu Y, Zhang J. Numerical simulation and optimization of sinter cooler in multilayered burden distribution. Journal of Central South University (Science and Technology), 2013, 44(3): 1228-1234. (in Chinese).
[33] Xia J, Zeng Q. Numerical simulation of sinter cooling in ring cooler. Microcomputer Information, 2010, 26(11): 98-100. (in Chinese).
[34] Liu Y, Wang J,Yuan X. Numerical investigation of flow and heat transfer of sinter cooling process in annular cooler. Proceeding of Academic Conference of Chinese Society of Engineering Thermophysics, paper No. 123531, Dongguan, 2012. (in Chinese).
[35] Zheng K C, Wen Z, Liu X C. Investigating the general mathematics model of gas-solid heat transfer in the cooling process of high temperature clinker and sintered material. Energy for Metallurgical industry, 2010, 29(2): 27-30. (in Chinese).
[36] Liu B, Feng H, Jiang Z. Heat and mass transfer in sintering process. Journal of Chemical Industry and Engineering (China), 2012, 63(5): 1344- 1353. (in Chinese).
[37] Nield D A, Bejan A. Convection in Porous Media (4th edition). New York: Springer, 2012.
[38] Ergun S. Fluid flow through packed column. Chemical Engineering Process, 1952, 48(2): 89-94.
[39] Kye S H, Jae H J, Won K I. Fixed-bed adsorption for bulk component system: non- equilibrium non-isothermal and non-adiabatic model. Chemical Engineering Science, 1995, 50(5): 813-825.
[40] Zhou J. Heat Transfer. Beijing: Metallurgical Industry Press, 1999. (in Chinese).
[41] Xu R. Research on the Basic Theory of Sintering process: Modeling and Simulation. PhD Thesis, Beijing: Beijing Institute of Iron and Steel Engineering, 1988. (in Chinese).
[42] Liu B. Numeral Analysis for Thermal Process of Sintering Machine and Annular Cooler. Master Thesis, Beijing: University of Science and Technology Beijing, 2010. (in Chinese).

Xun Shen received his BS Degrees in 2011 in engineering mechanics and aerospace engineering from the Tsinghua University, P R China. He is pursuing for his PhD Degree in power engineering and engineering thermophysics from Naval University of Engineering, P R China. His work covers topics in finite time thermodynamics and technology support for propulsion plants. BS Shen is the author or co-author of over 10 peer-refereed articles (1 in English).

Lingen Chen received all his degrees (BS, 1983; MS, 1986, PhD, 1998) in power engineering and engineering thermophysics from the Naval University of Engineering, P R China. His work covers a diversity of topics in engineering thermodynamics, constructal theory, turbomachinery, reliability engineering, and technology support for propulsion plants. He had been the Director of the Department of Nuclear Energy Science and Engineering, the Superintendent of the Postgraduate School, and the Dean of the College of Naval Architecture and Power. Now, he is the Direct, Institute of Thermal Science and Power Engineering, the Director, Military Key Laboratory for Naval Ship Power Engineering, the Direct of the National Experimental Teaching Demonstration Center for Naval Ship Power Engineering, and the Dean of the College of Power Engineering, Naval University of Engineering, P R China. Professor Chen is the author or co-author of over 1500 peer-refereed articles (over 655 in English journals) and 12 books (two in English).
E-mail address: lgchenna@yahoo.com; lingenchen@hotmail.com, Fax: 0086-27-83638709 Tel: 0086-27-83615046.

Shaojun Xia received all his degrees (BS, 2007; PhD, 2012) in power engineering and engineering thermophysics from the Naval University of Engineering, P R China. His work covers topics in finite time thermodynamics and technology support for propulsion plants. Dr. Xia is the author or co-author of over 50 peer-refereed papers (over 35 in English journals).

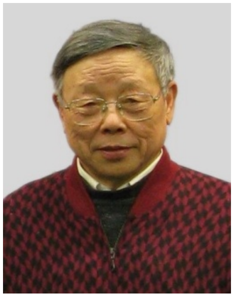

Fengrui Sun received his BS Degrees in 1958 in Power Engineering from the Harbing University of Technology, P R China. His work covers a diversity of topics in engineering thermodynamics, constructal theory, reliability engineering, and marine nuclear reactor engineering. He is a Professor in the College of Power Engineering, Naval University of Engineering, P R China. Professor Sun is the author or co-author of over 870 peer-refereed papers (over 450 in English) and two books (1 in English).

